JPET Fast Forward. Published on March 23, 2009 as DOI: 10.1124/jpet.109.152058
This article has not been copyedited and formatted. The final version may differ from this version.

Title Page

Differential Localization of Flavin-Containing Monooxygenase Isoforms 1, 3, and 4 in Rat Liver and Kidney and Evidence for Expression of FMO4 in Mouse, Rat, and Human Liver and Kidney Microsomes

Rachel M. Novick, Ann M. Mitzey, Mark S. Brownfield, Adnan A. Elfarra*

Department of Comparative Biosciences (R.M.N., A.M.M., M.S.B., A.A.E.) and Molecular and Environmental Toxicology Center (R.M.N., A.A.E.), University of Wisconsin-Madison, Madison, WI 53706

Running Title Page

Localization of FMO1, 3, and 4 in rat liver and kidney

Corresponding author:

Dr. Adnan Elfarra

School of Veterinary Medicine

2015 Linden Drive

Madison, WI 53706

Tel: (608) 262-6518

Fax: (608) 263-3926

Email: elfarraa@svm.vetmed.wisc.edu

Text pages: 27

Number of Tables: 2

Number of Figures: 7

Number of References: 39 (<40)

Abstract Words: 247 (<250)

Introduction Words: 631 (<750)

Discussion Words: 1532 (<1500)

Abbreviations: FMO, flavin-containing monooxygenase; IHC, immunohistochemistry; PV, perivenous; PP, periportal; DT, distal tubules; PT proximal tubules; PBS, phosphate buffered saline; DCVC, *S*-(1,2-dichlorovinyl)-L-cysteine

Section: Metabolism, Transport, and Pharmacogenomics

JPET Fast Forward. Published on March 23, 2009 as DOI: 10.1124/jpet.109.152058
This article has not been copyedited and formatted. The final version may differ from this version.

Abstract

Flavin-containing monooxygenases (FMOs) play significant roles in the metabolism of drugs and endogenous or foreign compounds. In this study, the regional distribution of FMO isoforms 1, 3, and 4 were investigated in male Sprague- Dawley rat liver and kidney using immunohistochemistry (IHC). Rabbit polyclonal antibodies to rat FMO1 and FMO4, developed using antipeptide technology, and commercial anti-human FMO3 antibody were used; specificities of the antibodies were verified using western blotting, immunoprecipitation, and IHC. In liver, the highest immunoreactivity for FMO1 and FMO3 was detected in the perivenous region and decreased in intensity toward the periportal region. In contrast, FMO4 immunoreactivity was detected with the opposite lobular distribution. In the kidney, the highest immunoreactivity for FMO1, 3, and 4 was detected in the distal tubules. FMO1 and FMO4 immunoreactivity was also detected in the proximal tubules with strong staining in the brush borders, whereas less FMO3 immunoreactivity was detected in the proximal tubules. Immunoreactivity for FMO3 and FMO4 was detected in the collecting tubules in the renal medulla and the glomerulus, whereas little FMO1 immunoreactivity was detected in these regions. The FMO1 antibody did not react with human liver or kidney microsomes. However, the FMO4 antibody reacted with male and female mouse and human tissues. This data provided a compelling visual demonstration of the isoform-specific localization patterns of FMO1, 3 and 4 in the rat liver and kidney and the first evidence for expression of FMO4 at the protein level in mouse and human liver and kidney microsomes.

Introduction

Flavin-containing monooxygenases (FMOs) are microsomal enzymes that catalyze oxidation of pharmaceutical drugs, pesticides, and endogenous compounds. Generally, FMO oxidation increases the polarity of substrates aiding in excretion and detoxification; however, some substrates are bioactivated to reactive or toxic metabolites. Five expressed FMO isoforms (FMO 1-5) have been detected in humans (Lawton et al., 1994). FMO isoforms have different substrate selectivity and exhibit distinct sex-, tissue-, age-, and species-dependent expression profiles (Hines et al. 1994).

The liver typically contains the largest concentrations of xenobiotic metabolizing enzymes. Adult human liver mRNA exhibits high FMO3 expression, moderate FMO4 expression, and extremely low FMO1 expression (Cashman and Zhang, 2006; Dolphin et al., 1996). In contrast, rat or mouse liver has moderate FMO1 protein expression (Falls et al., 1995; Lattard et al., 2002). To our knowledge, FMO localization in liver has been elucidated only in mice by in situ hybridization (Janmohamed et al., 2004). FMO1 and FMO5 mRNAs were detected across the acinus with a concentration gradient decreasing from the perivenous (PV) to the periportal (PP) hepatocytes. FMO2, 3 and 4 mRNAs were localized heavily in the PP region (Janmohamed et al., 2004). The heterogeneous expression patterns of FMO isoforms within the liver may suggest distinct roles in metabolism of drugs, xenobiotics, and endogenous compounds.

The kidney plays a large role in extrahepatic metabolism due to high exposure via perfusion and potential concentration of substrates within the tissue. Regions of the kidney, such as the proximal tubules (PT), may have a high density of xenobiotic metabolizing enzymes (Lock and Reed, 1998). In human kidney, mRNA expression

levels are high for FMO1, moderate for FMO4 and low for FMO3 (Dolphin et al., 1996; Zhang and Cashman, 2006). In the rat, FMO3 mRNA expression is greater in the kidney than the liver (Burnett et al., 1994; Lattard et al., 2001). In male and female mouse kidney, FMO1, 2, 3, 4, and 5 mRNAs were localized to the PT and distal tubules (DT) of the cortex, and the collecting tubules of the renal medulla; whereas only FMO1 mRNA was detected in the glomeruli (Janmohamed et al., 2004). In male rat kidneys, immunoreactivity with antibodies to rabbit lung FMO2 was localized in the PT and DT of the renal cortex and the collecting ducts of the renal medulla, but was not detected in the glomeruli (Bhamre et al., 1993).

Previously, FMO3 and FMO5 mRNA levels did not correlate with FMO isoform protein levels in human liver samples (Overby et al., 1997). mRNA levels are not always well correlated to protein expression due to transcript instability and post-transcriptional regulation. Thus, in the present study we used antibodies to FMO1, FMO3, and FMO4 to assess protein expression levels. We focused on these isoforms because of their known or suspected greater metabolic activities in comparison with FMO2 and FMO5.

Moderate FMO4 mRNA levels were detected in the liver and kidney in many mammalian species including rat and human (Burnett et al., 1994; Cashman and Zhang, 2006; Nishimura and Naito, 2006). The expression of truncated or mutated human FMO4 in a heterologous system resulted in a protein that is metabolically active with methimazole, *S*-allyl-L-cysteine and L-methionine (Itagaki et al., 1996; Krause et al., 2003; Ripp et al., 1999). Because of the potential biological activity of FMO4 and its moderate expression, we included this isoform in our IHC studies. Previously, tissue-specific expression of two FMO4 variants was characterized in rat brain and kidney by

western blot using two different antibodies to rat FMO4 peptides (residues 126-140 and 409-423 of the deduced FMO4 long form (Lattard et al., 2003). The detection of FMO4 in rat tissue is the only protein level examination of FMO4. Thus, we used the FMO4 anti-peptide antibody to examine the protein expression of FMO4 in mouse and human liver and kidney microsomes.

Methods

Materials. Human cDNA-expressed FMO1, 3, and 5 and anti-human FMO3 antibody were purchased from BD Biosciences (Woburn, MA). Protein A plus and disuccinimidyl suberate crosslinker were purchased from ThermoFisher Scientific (Waltham, MA). For IHC studies, adult male Sprague-Dawley rats (300 g) were purchased from Jackson (Bar Harbor, ME) or Harlan (Madison, WI). Adult male and female $B6C3F_1$ mice were purchased from Jackson. Animals were maintained on a 12 hr light/dark cycle with free access to food and water. For western blots and immunoprecipitation experiments male Sprague-Dawley rat liver and kidney were purchased from Pel-Freez (Rogers, AR), human liver samples from adult Caucasians were purchased from SRI International (Menlo Park, CA), and human kidney samples from adult Caucasians were procured from International Bioresearch Solutions (Pasadena, CA). All tissues were made into "washed" microsomes by standard methods (Sausen and Elfarra, 1990). Protein concentrations were determined using the bicinchoninic acid assay (ThermoFisher Scientific) using bovine serum albumin as the standard.

Antibodies: Antibodies were produced against synthetic peptides derived from the predicted sequence of rat FMO1 and FMO4. Full length amino acid sequences were obtained from the National Center for Biotechnology Information and subjected to computer analysis using GeneRunner. A peptide from each protein was selected for antibody production based on indices of antigenicity, surface probability, and structural complexity. Database homology analysis using BLASTp (National Center for Biotechnology Information) confirmed the specificity of these candidate antigens for

each rat FMO isoform. Chosen peptides were: rat FMO1 (403-423) and rat FMO4 (long form Cys-415-434; corresponding to Cys-352-371 of the short form). Cysteine was used as a crosslinking site. For peptides without Cys in their sequence Cys was added to the N-terminal and all peptides were acetylated at the N terminus and amidated at the C terminus. The immunogen consisted of synthesized peptides crosslinked to keyhole lympet hemocyanin (Open Biosystems: Huntsville, AL). For each peptide immunogen two New Zealand white rabbits were subcutaneously injected with 0.50 mg of antigen at 10 sites. Subcutaneous booster injections of 0.25 mg of antigen at 4 sites were performed on day 14, 28, and 42. Antisera were harvested on day 56, 72 and throughout a three month period (Open Biosystems).

Antisera were purified by column affinity chromatography against the synthetic peptides. Affinity matrices were prepared using Sulfolink^{T} media (ThermoFisher Scientific) according to the manufacturer's protocol. To purify the antisera, samples were diluted with equal amounts of 10 mM Tris, pH 7.5 and pumped through the 1 mL column with the same buffer resulting in the elution of a large protein peak. Next, the column was washed to elute loosely adhering protein with 10 mM Tris-0.5 M sodium chloride, pH 7.5. Purified antibody was eluted with 100 mM glycine, pH 2.5 or 100 mM acetic acid pH 4 into tubes containing an equal volume of 1 M Tris, pH 8. Protein fractions were monitored at 280 nm (ISCO, Lincoln, NE). Antibody containing fractions were pooled and dialyzed against 0.05 M phosphate buffered saline pH 7.4 (PBS), concentrated by centrifugal filtration, and stored with 1% bovine serum albumin and 0.1% sodium azide. Antisera were characterized by immunoblotting, immunoprecipitation, and immunohistochemistry as described below.

Immunoblotting: Antibodies were characterized by the immunoreactivity to proteins separated by SDS-PAGE (12.5% Tris Criterion precast gel, Bio Rad, Hercules, CA). Protein samples were diluted in activated sample buffer containing 2-mercaptoethanol. Immunoblots used for characterization of antibodies included prestained molecular weight standards (Bio-Rad), human cDNA-expressed FMO1, FMO3, and FMO5 (BD Biosciences, 1.5 µg), and rat liver and kidney microsomes (20 µg or 10 µg). Immunoblots for immunoprecipitation used rat kidney microsomes (10 µg) as the positive control and immoprecipitated samples (15 µl) to determine reactivity with the retained protein. Immunoblots used to determine species cross reactivity of the FMO4 antibody contained rat kidney (15 µg), rat liver (30 µg), human liver and kidney (15 µg), and mouse liver and kidney (30 µg) microsomal samples. The gels were run for 80 min with 200 V, and then transferred to Hybond-ECL nitrocellulose membrane (Amersham Biosciences, Piscataway, NJ) at 70 mAmps for 70 min. The nitrocellulose was incubated in blotting reagent (5% powdered milk, 0.06 M NaCl in 25 mM Tris pH 7.5) for 1 h and washed in Tris-buffered saline with 0.1% Tween-20 multiple times. The nitrocellulose was exposed overnight to primary antibody. For immunoblots with rat tissue, dilutions of 1:250 or 1:500 were used and for immunoblots with human or mouse tissue, dilutions of 1:250 or 1:100 were used. Blots were washed in Tris-buffered saline with 0.1% Tween-20 and incubated for 1 h with horseradish peroxidase conjugated goat anti-rabbit antibody (Jackson ImmunoResearch, West Grove, PA). After washing, blots were treated with West Pico Super Signal chemiluminescent substrate (ThermoFisher Scientific).

Immunoprecipitation: Purified antipeptide FMO1 and FMO4 antibodies or FMO3 antibody (BD Biosciences) were bound to Protein A Plus (ThermoFisher

Scientific) by incubating together overnight at 4^{o}C. The bound antibodies were washed and cross linked according to manufacturer's instructions. Rat kidney microsomes were dialyzed against PBS, solubilized with 1% Triton-X 100, and pre-cleared by incubating (1-3 h) with Protein A Plus. The microsomes were incubated overnight at 4^{o}C with the antibody cross-linked to Protein A Plus. The unbound protein was washed off with PBS and the bound protein was eluted with ImmunoPure IgG Elution Buffer (150 μL; pH 2.8 ThermoFisher Scientific). The eluted protein was immediately neutralized with 1 M Tris pH 9.5. Eluted samples were then run by SDS-PAGE and immunoblotted as described above.

Immunohistochemistry. Male Sprague-Dawley rats were deeply anesthetized with isofluorane and then sodium pentobarbital (60 mg/kg ip), thoracotomized and the right atrium was opened and the left ventricle cannulated. Rats were then perfused intracardially with a flush solution (Tyrrodes solution containing 0.1% heparin and 0.2% procaine), followed by a histological fixative (4% paraformaldehyde with 0.1% glutaraldehyde in 0.1 M phosphate buffer, pH 7.5). Liver and kidney blocks were removed and fixed overnight in the same fixative at 4^{o}C. Tissues were dehydrated in ascending concentrations of ethanol, xylene, and finally embedded in paraffin. Tissue sections (10 microns) were cut on a rotary microtome and sections were mounted on gelatin subbed slides.

Sections were deparaffinized with xylene and rehydrated with descending concentrations of ethanol to PBS, to prepare the tissue for IHC processing. Sections were incubated in 0.5% hydrogen peroxide in methanol (30 min) to quench endogenous peroxidase activity and washed. Then, sections were subjected to an antigen retrieval

protocol where sections were incubated in 10 mM citric acid (85^{o}C for 10 min), cooled, and washed in PBS. This procedure results in intensified staining. Sections were immunohistochemically stained using a proprietary polymer based peroxidase staining method (Biocare Medical; Concord, CA). Sections were first subjected to a blocking step for 5 min in "Background Sniper", washed in IHC buffer (0.05 M PBS pH 7.4 with 0.1% gelatin, 0.002% neomycin and 5% normal goat serum) and incubated in diluted 1:25-1:200 anti-peptide FMO antibodies in IHC buffer overnight in the refrigerator. Slides were drained and washed in IHC buffer and processed for bound antibody detection by incubation in full strength Biocare MACH2 Polymer-HRP conjugate for 30 min, washed in 0.05 M PBS, 0.1 M Tris, pH 7.5, developed with diaminobenzidene (30 mg), hydrogen peroxide (0.01%), and nickel ammonium sulfate (0.02%) for 7-10 min, washed in 0.1 M Tris pH 7.5, PBS, dehydrated in ethanol, cleared in xylene, and mounted with a coverslip with Permount^{T} (ThermoFisher Scientific).

Control IHC studies included processing of tissue with omitted, soluble, or solid matrix immunoabsorbed anti-FMO antibodies. Control tissues were run in parallel with antibody incubated tissues. Sections were viewed using a Nikon Eclipse-600 photomicroscope equipped with a Spot^{T} digital camera (Diagnostic Products, Sterline Hts, MI). Photographs were quality-enhanced using Paint Shop (Corel, Ottawa, Canada).

Results

Characterization of the specificity of the FMO1, FMO3, and FMO4 antibodies: To our knowledge, no commercial antibodies are available for rat FMO1, 3 or 4. We produced rabbit polyclonal antibodies to rat FMO1 and FMO4 by selecting rat FMO1 and FMO4 peptides based upon their high degree of antigenicity, surface probability, and structural complexity. The selected peptides underwent a BLASTp search and were unique to the FMO isoform. Prior to use rabbit antisera were purified by column affinity chromatography against the synthetic peptides to increase specificity and purity of the antibodies. The antipeptide FMO1 antibody reacted strongly with rat liver and kidney microsomes at the approximate molecular weight of FMO1 (~60 kDa) but not with cDNA-expressed human FMO1, 3, and 5 (Fig. 1). The antipeptide FMO4 antibody reacted with rat liver and kidney microsomes but not with cDNA-expressed human FMO1, 3, and 5 (Fig. 1). In some immunoblots, rat liver microsomal protein exhibited two bands at a slightly different electrophoretic mobilities (56 KDa and 63 KDa; Fig 7). Commercial anti-human FMO3 detected the orthologous rat protein and was used in this study (Fig. 1). Anti-human FMO3 antibody (BD Biosciences) reacted with cDNA-expressed human FMO3 and rat liver and kidney microsomes at the approximate molecular weight of FMO3 (~60 kDa) but not with cDNA-expressed human FMO1 and FMO5 (Fig 1).

Immunoprecipitation of FMO1, 3, and 4 was done by crosslinking the antibodies to protein A and incubating with 1% triton-X 100 solubilized rat kidney microsomes. The immunoprecipitated sample for each antibody was run by SDS-PAGE and immunoblotted with the antibody used in immunoprecipitation. A band at the

approximate molecular weight of FMOs was detected indicating the respective FMO was retained by the antibody (Fig. 2). Denaturation by SDS was not necessary as the antibodies were able to react with the native FMO protein as indicated by the immunoprecipitation and IHC results (discussed below).

During IHC, titration studies of anti-FMO3, FMO1, and FMO4 antipeptide antibodies yielded staining patterns in liver and kidney that were diminished by dilution. For FMO1 and FMO4 antipeptide antibodies the three parallel control experiments with omitted, soluble, or solid matrix absorbed antibody resulted in a complete loss of staining (Fig. 3, Fig. 4C, Fig. 6D). Also, there appeared to be no difference between staining results within the pairs of antibodies produced in individual rabbits for each FMO isoform.

Localization of FMO1, FMO3, and FMO4: Liver immunoreactivity showed a reverse intralobular distribution for FMO1 and FMO3 versus FMO4 (Fig. 3). FMO1 and FMO3 immunoreactivity was centered around the PV region at the interior of the liver lobules, gradually diminishing radially from this site. The distribution of immunoreactivity to FMO4 antipeptide antibody was the reverse, with higher concentration near the periacinus regions at the corners of the lobules and gradually diminishing toward the central PV region. FMO1 and FMO4 antibodies that were exposed to the affinity column matrix containing the synthesized peptide did not exhibit any staining patterns in the liver (Fig. 3).

Sections of the kidney cortex showed a large number of stained renal tubules among other unstained tubules for FMO1 (Fig. 4), FMO3 (Fig. 5), and FMO4 (Fig. 6). Cortical staining was equally immunopositive for all three FMO isozymes in the DT. In

this site, intense staining filled the cells' cytoplasm and close perinuclear region, suggestive of reactivity in the Golgi apparatus. Immunoreactivity was also seen in the PT, but its intensity and distribution varied between the three isoforms. The brush border was most intensely stained for FMO1 (Fig. 4A), slightly less for FMO4 (Fig. 6A), and very faintly or not at all for FMO3 (Fig. 5B). FMO3 staining of the PT showed regional differences with the S1 segment staining lightly or not at all, the S2 segment staining more densely, and the S3 segment staining most densely. PT cells reacting with FMO1 had strong intracellular body immunoreactivity, but lightly to moderately stained cytoplasm (Fig. 4A). For FMO4 there were densely stained basal bodies but the cytoplasmic staining was weak (Fig. 6A). Staining for FMO1 was absent in the kidney medulla, but strong in kidneys reacted with antisera to FMO3 (Fig. 5A, 5C) and FMO4 (Fig. 6C). This staining was attributed to strong collecting tubule immunoreactivity (Fig. 5C, 6C). Glomeruli showed immunoreactivity for FMO3 (Fig. 5B) and FMO4 (Fig. 6A), but not FMO1 (Fig. 4A). FMO3 glomerular immunoreactivity was strongest (Fig. 5B inset). FMO4 immunoreactivity was strong in the renal papilla showing striations of the tubules feeding into it from the outer zone of the medulla (Fig. 6B). The immunoabsorbed controls for FMO1 and FMO4 exhibited a complete loss of staining (Fig. 4C, Fig. 6D). The immunohistochemical findings are summarized in Table 1.

Antibody crossreactivity in human and mouse tissues: The FMO1 and FMO4 antipeptide antibodies were tested for immunoreactivity in male and female mouse and human liver and kidney microsomes. The antipeptide FMO4 antibody reacted with mouse and human liver and kidney microsomes (Fig. 7). The bands of immunoreactivity in mouse and human tissues exhibited the same electrophoretic mobility as the band

characterized in rat kidney. Male and female rat liver exhibited an immunoreactive band at a slightly lower molecular mass (~56 kDa) than the band in rat kidney (~63 kDa) corresponding to the predicted molecular mass of the short and long splicing variants of FMO4 (Fig. 7). Low antibody dilutions were used to detect mouse FMO4 which may have resulted in detection of protein degradation or aggregation products exhibited in this immunoblot (Fig.7). FMO1 antipeptide antibody did not react with human liver and kidney microsomes, consistent with the lack of reactivity of the antipeptide FMO1 antibody with human cDNA-expressed FMO1 (Fig. 1). When we immunoblotted the FMO1 antibody against microsomal protein from male and female mouse liver and kidney (15 μg) no reaction was observed. However, weak cross reaction of rat antipeptide FMO1 was observed in male mouse liver and kidney at high protein loads (40 μg) and low antibody dilution (1:50; data not shown).

Discussion

The localization of FMO1, FMO3, and FMO4 in male rat liver and kidney was characterized to assess the potential role of different FMO isoforms in drug and toxicant metabolism and toxicity. FMO1 and FMO4 antibodies were produced against a synthetic peptide with unique homology to each FMO isoform. The immune sera was affinity purified with the peptide to increase specificity. Immunoblotting showed reactivity at the correct molecular weight and lack of reactivity against alternate human cDNA expressed FMO isoforms. Characterization of the antibodies by immunoprecipitation and by IHC controls provide further evidence the exhibited immunoreactivity is isoform specific.

The localization of FMO1 and FMO3 in the PV region in male rat liver is similar to the localization of P450s (Lindros, 1997). Previously, FMO3 mRNA in male mouse liver was reported to have the opposite intralobular distribution using in situ hybridization methods (Janmohamed et al., 2004). While differences between the methods used in these studies complicate the comparison, the difference in FMO3 localization between rats and mice is supportive of the hypothesis that FMO3 expression is regulated differently between the two rodent species as indicated by the difference in testosterone regulation (Falls et al., 1997; Lattard et al., 2002). The FMO4 localization pattern in the PP region is similar to phase II enzymes, such as glutathione peroxidase (Lindros, 1997). FMO4 localization in the PP region may cause the liver acinus to be selectively exposed to FMO4 metabolites, which could protect the liver or increase exposure to reactive metabolites.

The differential patterns of FMO expression in the liver lobule are important for the toxicological evaluation of FMO mediated substrates. In this regard, ketoconazole has

been documented to cause hepatoxicity and liver necrosis in the PV region (Stricker et al., 1986). Because the hepatotoxicity of ketoconazole is caused in part by an FMO3 metabolite (Rodriguez and Acosta, 1997; Rodriguez and Miranda, 2000), our localization of FMO3 to the PV region suggests FMO3 may play a role in the zonal selectivity of ketoconazole necrosis.

Liver zonal heterogeneity between isoforms may be due to the microenvironment of hepatocytes which are exposed to different levels of hormones and xenobiotic inducers. Little is known about how FMO zonation is regulated and if it is modified with endogenous or exogenous signals. FMO expression is affected by testosterone and estrogen exposure (Falls et al., 1997) and by foreign compounds such as 2,3,7,8,-tetrachlorodibenzo-p-dioxin, 3-methylchlorathane, and rantidine (Celius et al., 2008; Chung et al., 1997; Rae et al., 2001; Tijet et al., 2006). Interestingly, individual P450s respond to inducers in the rat liver acinus in a region-dependent manner, generally being induced in the same area that the isozyme is constitutively expressed (Buhler et al., 1992). Further investigation is needed to determine if FMO localization patterns will change in response to endogenous or exdogenous signals.

The IHC localization of FMO1, 3, and 4 immunoreactivity in the DT of renal cortex (Fig. 4A, 5B, 6A) is consistent with the localization of other xenobiotic metabolizing enzymes, including many isoenzymes in the P450 family (Cummings et al., 1999). In mice FMO1, 2, 3, 4, and 5 mRNA were all primarily localized to the distal tubules of the cortex (Janmohamed et al., 2004). Consistent with our results (Fig. 4A) *S*-benzyl-L-cysteine *S*-oxidase activity, primarily an FMO1 mediated reaction, was greater in isolated rat DT cells than PT cells (Lash et al., 1994).

The PT brush border is on the luminal surface of the epithelial cells and is involved in the reabsorbtion of the solutes in the filtrate through metabolically driven transport. This action can increase the concentration of many xenobiotics, thus, the PT plays a large role in chemical bioactivation and is highly susceptible to chemical insult. Many xenobiotic metabolizing enzymes are localized in the PT cells including P450s and glutathione transferase (Lock and Reed, 1998) and some have been localized to the PT epithelial cells (Murray, 1999; Muskhelishvili, 2001). This area stained most intensely for FMO1, followed by FMO4, and faintly for FMO3 (Fig. 4A, 5B, 6A). This suggests the PT may be more sensitive to the substrates metabolized by FMO1 such as thiourea and hydrazines (Reviewed in Krueger and Williams, 2005).

The glomerulus is the entrance to the kidney and FMO localization in this region would expose the rest of nephron to FMO metabolites. In our study, immunoreactivity to FMO3 and FMO4 was detected in the glomeruli and in the collecting tubules in the renal medulla. Interestingly in mice all five FMO mRNAs were detected in the collecting ducts of the medulla and only FMO1 mRNA was detected in the glomeruli (Janmohamed et al., 2004).

The FMO3 substrate *S*-(1,2-dichlorovinyl)-L-cysteine (DCVC) (Krause et al., 2003; Ripp et al., 1997), a metabolite of trichloroethylene, is a rat nephrotoxin. The S3 segment of the proximal tubules is the most sensitive area to DCVC and the more potent FMO mediated metabolite DCVC sulfoxide (Jones et al., 1988; Lash et al., 1994). Interestingly, we found FMO3 to be more heavily localized in the S3 region of the PT cells than the S2 or S1 region indicating FMO3 may play a role in DCVC-induced toxicity. The greater sensitivity of the S3 segment of the proximal tubules could also be

due to selective accumulation of DCVC and DCVC sulfoxide in the PT (Zhang and Stevens, 1989). In vitro studies have shown DCVC sulfoxide plays a role in DCVC toxicity in human PT cells (Lash et al., 2003).

The direct detection of FMO4 at the protein level in human and mouse tissue is novel (Fig. 7). This data confirms mRNA detection at moderate or low expression levels in human liver and kidney (Cashman and Zhang, 2006; Dolphin et al., 1996; Lattard et al., 2004; Nishimura and Naito, 2006). Previously, mRNA FMO4 transcripts were not detected in the liver of adult male CD-1 mice (Falls et al., 1995) but low levels of FMO4 mRNA were detected in male and female 129/SV mice (0-8 weeks). Our detection of FMO4 in adult male and female mouse liver shows that FMO4 is expressed in this species and that there may be strain- or age- related differences in expression. Interestingly, the immunoreactivity in rat liver was of different electrophoretic mobility than the immunoreactivity in rat kidney, mouse liver and kidney and human liver and kidney (Fig. 7). This difference in molecular mass could be due degradation of the sample, post-translation modifications, or to tissue-specific splicing of the protein as was observed with rat brain and kidney (Lattard et al., 2003). Our observed molecular mass of 56 kDa for rat liver and 63 kDa for rat kidney (Fig. 7) are consistent with the predicted molecular mass of 55,871 Da for the short form of rat FMO4 and 63,395 for the long form of rat FMO4 (Lattard et al., 2003). A tissue-specific splicing variant could be indicative of functional change and warrants further investigation.

Notably, the FMO4 antibody reacted with mouse and human tissue whereas the FMO1 antibody did not react well with mouse or human tissue. A BLASTp search for the rat FMO1 peptide (residues 403-423) matched 20/21 amino acids in mouse FMO1 and

14/21 in human FMO1. A BLASTp for the rat FMO4 peptide (415-434 long form) matched 19/20 in mouse FMO4 and 15/20 human FMO4 (Table 2). There is one amino acid difference between the synthesized peptide for FMO1 and FMO4 and the mouse amino acid sequences yet the FMO4 antibody has a stronger reaction with mouse tissue than the FMO1 antibody. The rat FMO4 synthesized peptide contains a serine residue where there is a threonine residue in the mouse protein. Because both amino acids are polar with hydrophilic properties the structure of the peptides may not be significantly different. On the other hand, rat FMO1 peptide has lysine, a basic residue, switched to glutamic acid, an acidic residue, in the mouse protein. This change may alter the structure of the protein affecting its reactivity with the antibody. Human FMO4 has five amino acid differences from the rat peptide but still reacts with the antibody. The changed residues include isoleucine and leucine to phenylalanine which are all hydrophobic residues; glutamine to lysine which have amphipathic or hydrophilic character; and phenylalanine to tyrosine which have larger ring structures. There are seven amino acid differences between human and rat FMO1 synthesized peptide, and the anti-peptide antibody does not react with the human FMO1 protein. The residues that are different may cause structural changes such as glycine to tryptophan which is a large change in the size of the side chain and histidine to proline, as proline's ring structure restricts conformational freedom. Ultimately, the determination of antibody reactivity remains empirical as it is difficult to predict how the antibody is reacting with the protein and which amino acid changes will affect reactivity.

This study characterized FMO isoform specific antibodies, immunochemically localized FMO in rat liver and kidney and provided the first detection of FMO4 protein in

human and mouse liver and kidney. The localization patterns detected in rat tissues correspond to other xenobiotic metabolizing enzymes showing FMOs are optimally situated within the organ to act on foreign compounds. The potential species-specific difference between rats and mice are discussed and further investigation is needed to determine the role of FMO-mediated reactions in toxicity.

References

Bhamre S, Shankar SK, Bhagwat SV, Ravindranath V. (1993) Catalytic activity and immunohistochemical localization of flavin-containing monooxygenase in rat kidney. *Life Sci* **52**:1601-1607.

Buhler R, Lindros KO, Nordling A, Johansson I, Ingelman-Sundberg M. (1992) Zonation of cytochrome P450 isozyme expression and induction in rat liver. *Eur J Biochem* **204**:407-412.

Burnett VL, Lawton MP, Philpot RM. (1994) Cloning and sequencing of flavin-containing monooxygenases FMO3 and FMO4 from rabbit and characterization of FMO3. *J Biol Chem* **269**:14314-14322.

Cashman JR and Zhang J. (2006) Human flavin-containing monooxygenases. *Annu Rev Pharmacol Toxicol* **46**:65-100.

Celius T, Roblin S, Harper PA, Matthews J, Boutros PC, Pohjanvirta R, Okey AB. (2008) Aryl hydrocarbon receptor-dependent induction of flavin-containing monooxygenase mRNAs in mouse liver. *Drug Metab Dispos* **36**: 2499-2505.

Chung WG, Park CS, Roh HK, Cha YN. (1997) Induction of flavin-containing monooxygenase (FMO1) by a polycyclic aromatic hydrocarbon, 3-methylcholanthrene, in rat liver. *Mol Cells* **7**:738-741.

Cummings BS, Zangar RC, Novak RF, Lash LH. (1999) Cellular distribution of cytochromes P-450 in the rat kidney. *Drug Metab Dispos* **27**:542-548.

Dolphin CT, Cullingford TE, Shephard EA, Smith RL, Phillips IR. (1996) Differential developmental and tissue-specific regulation of expression of the genes encoding three members of the flavin-containing monooxygenase family of man, FMO1, FMO3 and FM04. *Eur J Biochem* **235**:683-689.

Falls JG, Blake BL, Cao Y, Levi PE, Hodgson E. (1995) Gender differences in hepatic expression of flavin-containing monooxygenase isoforms (FMO1, FMO3, and FMO5) in mice. *J Biochem Toxicol* **10**:171-177.

Falls JG, Ryu DY, Cao Y, Levi PE, Hodgson E. (1997) Regulation of mouse liver flavin-containing monooxygenases 1 and 3 by sex steroids. *Arch Biochem Biophys* **342**:212-223.

Hines RN, Cashman JR, Philpot RM, Williams DE, Ziegler DM. (1994) The mammalian flavin-containing monooxygenases: molecular characterization and regulation of expression. *Toxicol Appl Pharmacol* **125**:1-6.

Itagaki K, Carver GT, Philpot RM. (1996) Expression and characterization of a modified flavin-containing monooxygenase 4 from humans. *J Biol Chem* **271**: 20102-20107.

Janmohamed A, Hernandez D, Phillips IR, Shephard EA. (2004) Cell-, tissue-, sex- and developmental stage-specific expression of mouse flavin-containing monooxygenases (fmos). *Biochem Pharmacol* **68**:73-83.

Jones TW, Qin C, Schaeffer VH, Stevens JL. (1988) Immunohistochemical localization of glutamine transaminase K, a rat kidney cysteine conjugate beta-lyase, and the

relationship to the segment specificity of cysteine conjugate nephrotoxicity. *Mol Pharmacol* **34**:621-627.

Krause RJ, Lash LH, Elfarra AA. (2003) Human kidney flavin-containing monooxygenases and their potential roles in cysteine s-conjugate metabolism and nephrotoxicity. *J Pharmacol Exp Ther* **304**:185-191.

Krueger SK and Williams DE. (2005) Mammalian flavin-containing monooxygenases: structure/function, genetic polymorphisms and role in drug metabolism. *Pharmacol Ther* **106**: 357-387.

Lash LH, Putt DA, Hueni SE, Krause RJ, Elfarra AA. (2003) Roles of necrosis, apoptosis, and mitochondrial dysfunction in S-(1,2-dichlorovinyl)-L-cysteine sulfoxide-induced cytotoxicity in primary cultures of human renal proximal tubular cells. *J Pharmacol Exp Ther* **305**:1163-1172.

Lash LH, Sausen PJ, Duescher RJ, Cooley AJ, Elfarra AA. (1994) Roles of cysteine conjugate beta-lyase and S-oxidase in nephrotoxicity: Studies with S-(1,2-dichlorovinyl)-L-cysteine and S-(1,2-dichlorovinyl)-L-cysteine sulfoxide. *J Pharmacol Exp Ther* **269**:374-383.

Lattard V, Buronfosse T, Lachuer J, Longin-Sauvageon C, Moulin C, Benoit E. (2001) Cloning, sequencing, tissue distribution, and heterologous expression of rat flavin-containing monooxygenase 3. *Arch Biochem Biophys* **391**:30-40.

Lattard V, Lachuer J, Buronfosse T, Garnier F, Benoit E. (2002) Physiological factors affecting the expression of FMO1 and FMO3 in the rat liver and kidney. *Biochem Pharmacol* **63**:1453-1464.

Lattard V, Longin-Sauvageon C, Benoit E. (2003) Cloning, sequencing and tissue distribution of rat flavin-containing monooxygenase 4: Two different forms are produced by tissue-specific alternative splicing. *Mol Pharmacol* **63**:253-261.

Lattard V, Zhang J, Cashman JR. (2004) Alternative processing events in human FMO genes. *Mol Pharmacol* **65**:1517-1525.

Lawton MP, Cashman JR, Cresteil T, Dolphin CT, Elfarra AA, Hines RN, Hodgson E, Kimura T, Ozols J, Phillips IR. (1994) A nomenclature for the mammalian flavin-containing monooxygenase gene family based on amino acid sequence identities. *Arch Biochem Biophys* **308**:254-257.

Lindros KO. (1997) Zonation of cytochrome P450 expression, drug metabolism and toxicity in liver. *Gen Pharmacol* **28**:191-196.

Lock EA and Reed CJ. (1998) Xenobiotic metabolizing enzymes of the kidney. *Toxicol Pathol* **26**:18-25.

Murray GI, McFadyen MCE, Mitchell RT, Cheung Y-L, Kerr AC, Melvin WT (1999) Cytochrome P450 CYP3A in human renal cell cancer. *Br J Cancer* **79**: 1836-1842.

Muskhelishvili L, Thompson PA, Kusewitt DF, Wang C, Kadlubar FF. (2001) In situ hybridization and immunohistochemical analysis of cytochrome P450 1B1 expression in human normal tissues. *J Histochem Cytochem* **49**: 229-236.

Nishimura M and Naito S. (2006) Tissue-specific mRNA expression profiles of human phase I metabolizing enzymes except for cytochrome P450 and phase II metabolizing enzymes. *Drug Metab Pharmacokinet* **21**:357-374.

Overby LH, Carver GC, Philpot RM. (1997) Quantitation and kinetic properties of hepatic microsomal and recombinant flavin-containing monooxygenases 3 and 5 from humans. *Chem Biol Interact* **106**:29-45.

Rae JM, Johnson MD, Lippman ME, Flockhart DA. (2001) Rifampin is a selective, pleiotropic inducer of drug metabolism genes in human hepatocytes: Studies with cDNA and oligonucleotide expression arrays. *J Pharmacol Exp Ther* **299**:849-857.

Ripp SL, Overby LH, Philpot RM, Elfarra AA. (1997) Oxidation of cysteine S-conjugates by rabbit liver microsomes and cDNA-expressed flavin-containing mono-oxygenases: Studies with S-(1,2-dichlorovinyl)-L-cysteine, S-(1,2,2-trichlorovinyl)-L-cysteine, S-allyl-L-cysteine, and S-benzyl-L-cysteine. *Mol Pharmacol* **51**:507-515.

Ripp SL, Itagaki K, Philpot RM, Elfarra AA. (1999) Methionine S-oxidation in human and rabbit liver microsomes: evidence for a high-affinity methionine S-oxidase activity that is distinct from flavin-containing monooxygenase 3. *Arch Biochem Biophys* **367**: 322-332.

Rodriguez RJ and Acosta D,Jr. (1997) Metabolism of ketoconazole and deacetylated ketoconazole by rat hepatic microsomes and flavin-containing monooxygenases. *Drug Metab Dispos* **25**:772-777.

Rodriguez RJ and Miranda CL. (2000) Isoform specificity of N-deacetyl ketoconazole by human and rabbit flavin-containing monooxygenases. *Drug Metab Dispos* **28**:1083-1086.

Sausen PJ and Elfarra AA. (1990) Cysteine conjugate S-oxidase. characterization of a novel enzymatic activity in rat hepatic and renal microsomes. *J Biol Chem* **265**:6139-6145.

Stricker BH, Blok AP, Bronkhorst FB, Van Parys GE, Desmet VJ. (1986) Ketoconazole-associated hepatic injury. A clinicopathological study of 55 cases. *J Hepatol* **3**:399-406.

Tijet N, Boutros PC, Moffat ID, Okey AB, Tuomisto J, Pohjanvirta R. (2006) Aryl hydrocarbon receptor regulates distinct dioxin-dependent and dioxin-independent gene batteries. *Mol Pharmacol* **69**:140-153.

Zhang GH and Stevens JL. (1989) Transport and activation of S-(1,2-dichlorovinyl)-L-cysteine and N-acetyl-S-(1,2-dichlorovinyl)-L-cysteine in rat kidney proximal tubules. *Toxicol Appl Pharmacol* **100**:51-61.

Zhang J and Cashman JR. (2006) Quantitative analysis of FMO gene mRNA levels in human tissues. *Drug Metab Dispos* **34**:19-26.

Footnotes

This research is supported by National Institute of Health [Grants T32-ES-007015, RO1 DK044295]. Parts of this work were previously presented at the following conference: Novick RM, Mitzey AM, Brownfield BS and Elfarra AA (2009) Differential Localization of Flavin-Containing Monooxygenase Isoforms 1, 3, and 4 in Rat Liver and Kidney. Society of Toxicology Meeting; 2009 March 16; Baltimore, MD. Society of Toxicology, Reston, VA.

Legends for Figures

Figure 1. Immunoblotting to characterize FMO antibodies. Immunoblotting was performed as described in Materials and Methods and probed with rabbit polyclonal antipeptide FMO1 and FMO4 antibodies or anti-human FMO3 antibody. For all antibodies lanes 1-3 are cDNA-expressed human FMO1, FMO3, and FMO5 respectively (1.5 μg); lane 4 is rat liver microsomal protein (20 μg) and lane 5 is rat kidney microsomal protein (10 μg). Positions of molecular weight markers are shown.

Figure 2. Immunoprecipitation of FMOs from solubilized rat kidneys. FMOs were immunoprecipitated from rat kidney microsomal protein as described in Materials and Methods. Rat kidney microsomal protein (RK, 10 μg) and the eluted proteins (15 μL) were run by SDS-PAGE and immunoblotted by the antibody used to immunoprecipitate them. Positions of molecular weight markers are shown.

Figure 3. Immunoreactive FMO1, FMO3 and FMO4 in the liver lobule. The perivenous region (PV) at the center of the liver lobule and periportal (PP) sites at the periphery are labeled. Controls using immunoabsorbed anti-FMO antibodies are shown. Scale bar represents 100 μm.

Figure 4. Immunoreactive FMO1 in rat kidney. Proximal (PT) and distal tubules (DT) within a matrix of unstained glomeruli and tubulular elements are labeled. A control using immunoabsorbed FMO1 antibody is shown (C). Scale bar represents 50 μm (A) and 200 μm (B,C).

Figure 5. Immunoreactive FMO3 in rat kidney. Low power micrograph shows distribution of stained tubular elements in the cortex (A). At mid magnification these are shown to be primarily distal tubules (B). The glomerular immunoreactivity is shown (B, inset). Collecting tubules were also labeled. (C). Scale bar represents 200 μm (A, C) and 50 μm (B).

Figure 6. Immunoreactive FMO4 in rat kidney. Renal papilla (RP) are labeled as well as stained distal tubules (DT) and proximal tubules (PT) and collecting tubules (CT). A control using immunoabsorbed FMO4 antibody is shown (D). Scale bar represents 40 μm (A), 500 μm (B), 250 μm (C, D).

Figure 7. Immunoblotting with the FMO4 antipeptide antibody. Immunoblotting was performed as described in Materials and Methods with 15 μg of microsomal protein from male and female rat kidney and male and female human liver and kidney and 30 μg of microsomal protein from male and female rat liver and male and female mouse liver and kidney. The additional bands in the lower panel are likely due to the low antibody dilutions used which may have resulted in detection of protein degradation or aggregation products. Positions of molecular weight markers are shown.

JPET Fast Forward. Published on March 23, 2009 as DOI: 10.1124/jpet.109.152058
This article has not been copyedited and formatted. The final version may differ from this version.

Table 1: Immunohistochemical distribution of FMO isoforms in rat kidney and liver.

Immunohistochemical staining for each antibody was performed as described in Materials and Methods. The degree of staining was assessed in the following regions proximal tubules (PT), distal tubules (DT), collecting tubules (CT), glomeruli (Glom), and perivenous (PV) and periportal (PP). For the kidney sections the 1+ represents staining that is slightly above background and the 4+ represents the maximum density of staining. The 2+ and 3+ represent approximately 25% increments of increasing intensity between 1+ and 4+.

	Kidney				Liver	
Isoform	PT	DT	CT	Glom	PV	PP
FMO1	3+	4+	-	-	+	-
FMO3	1+	4+	3+	3+	+	-
FMO4	2+	4+	3+	1-2+	-	+

Table 2: Sequence homology between species for the synthesized peptides. Amino acids that are represented as bolded letters differ from the rat FMO sequence used to make the synthesized peptides.

FMO1 Peptide Sequence

Rat	403	SVMMKEVNERKKNKHSGFGLC	423
Mouse	403	SVMM**E**EVNERKKNKHSGFGLC	423
Human	403	SVM**IE**E**I**N**A**RK**E**NK**P**S**W**FGLC	423

FMO4 Peptide Sequence

Rat	415	KRGVIKDTSQDKLDFISYMD	434
Mouse	415	KRGVIKDTSQDKLDFI**T**YMD	434
Human	416	KRGV**F**KDTS**K**DK**F**D**Y**I**A**YMD	435

Figure 1

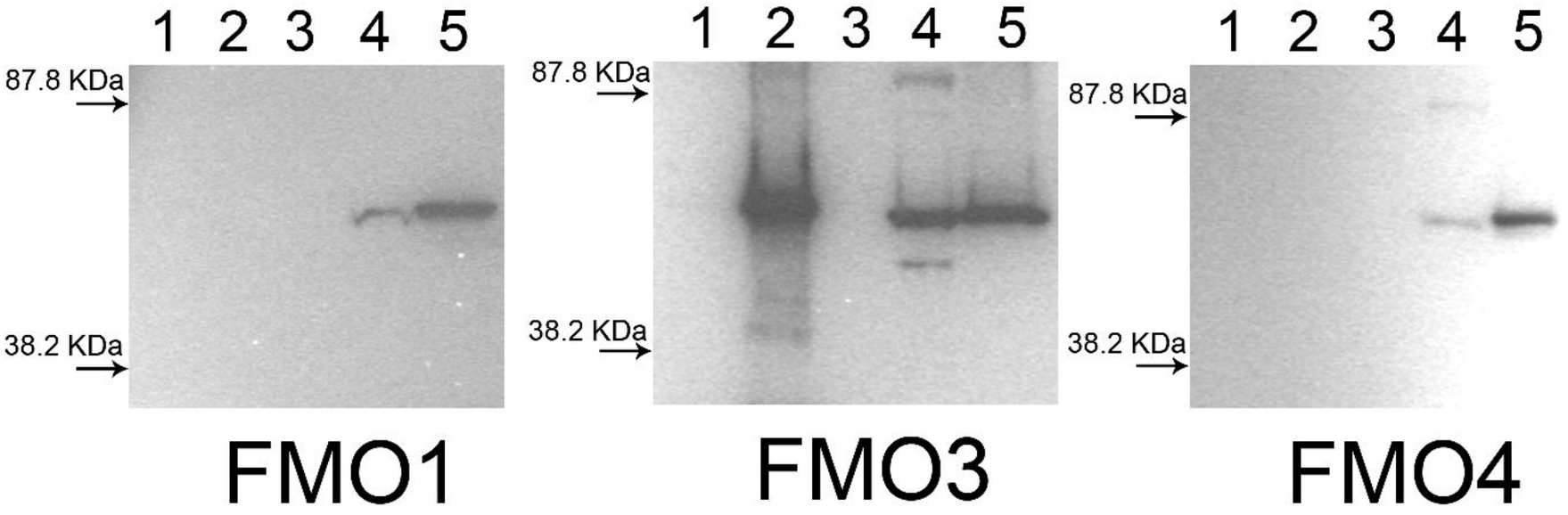
1 2 3 4 5
87.8 KDa
38.2 KDa
FMO1
1 2 3 4 5
87.8 KDa
38.2 KDa
FMO3
1 2 3 4 5
87.8 KDa
38.2 KDa
FMO4

Figure 2

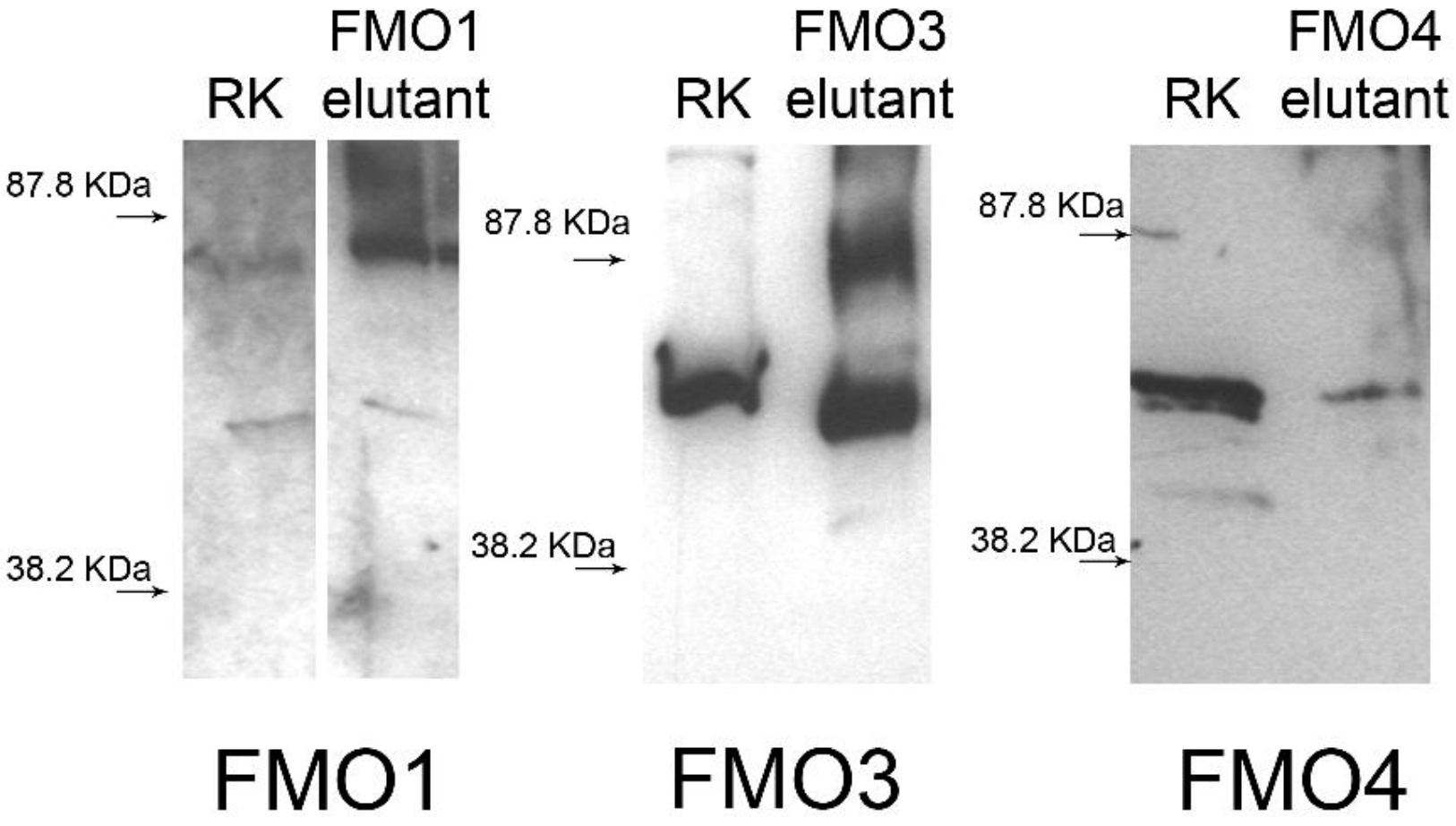
RK
FMO1 elutant
87.8 KDa
38.2 KDa
FMO1
RK
FMO3 elutant
87.8 KDa
38.2 KDa
FMO3
RK
FMO4 elutant
87.8 KDa
38.2 KDa
FMO4

Figure 3

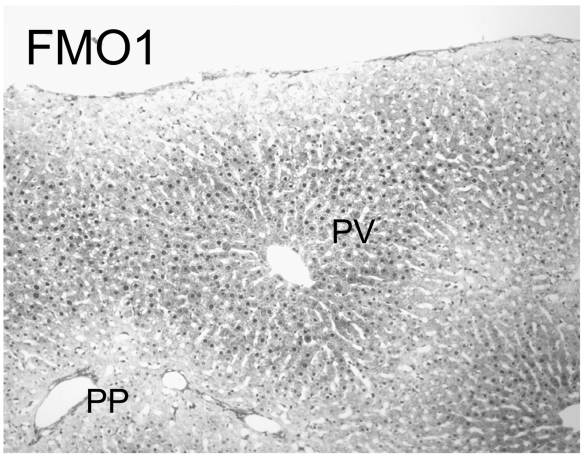

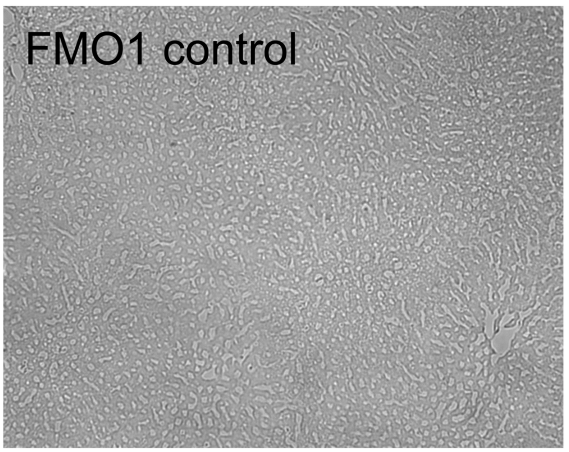

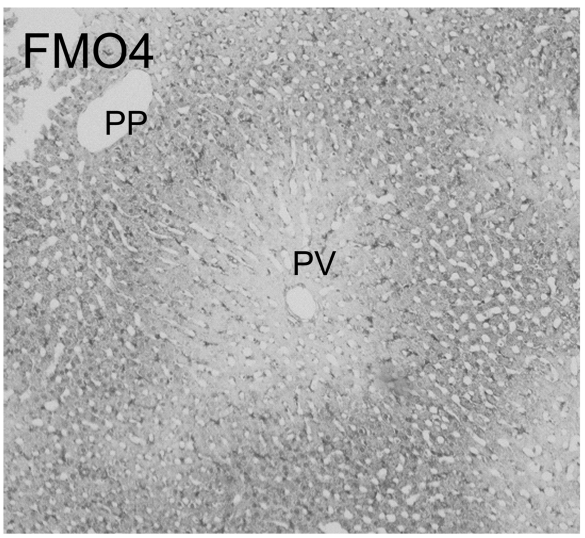

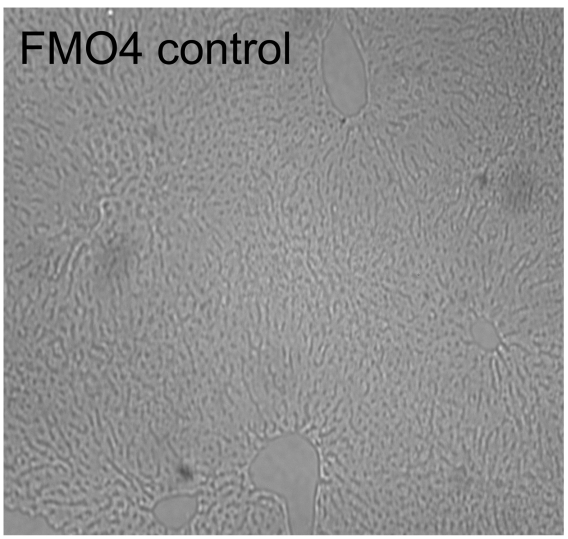

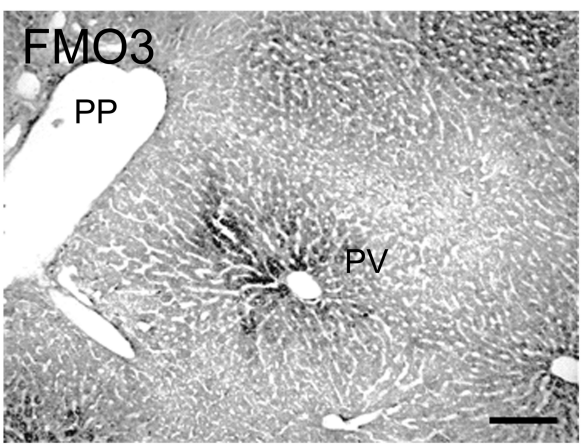

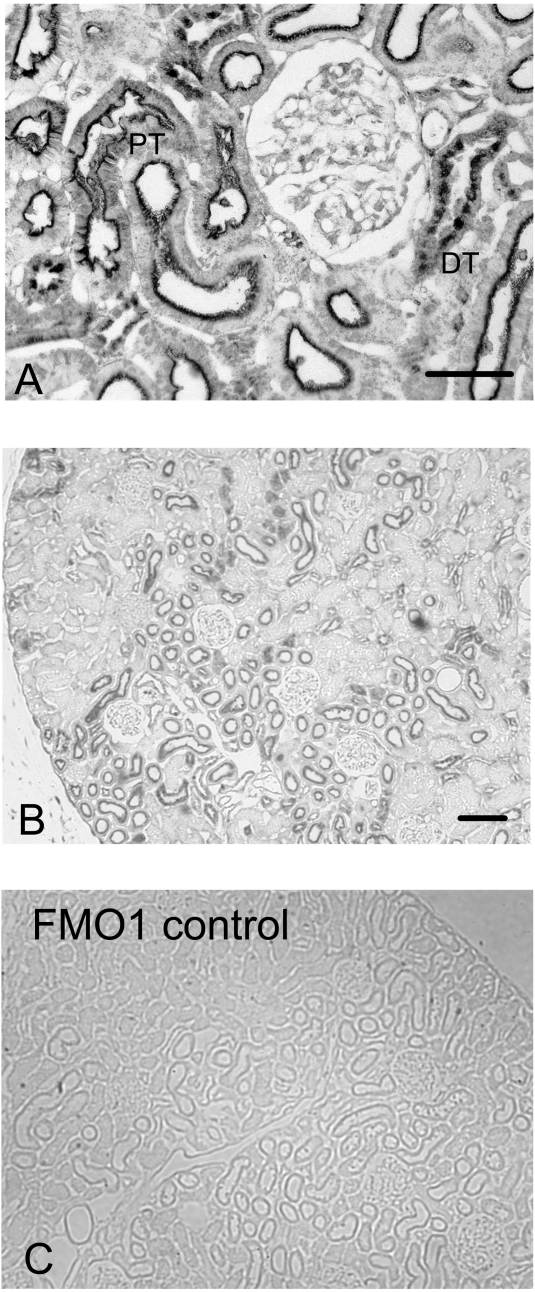

Figure 4

Figure 5

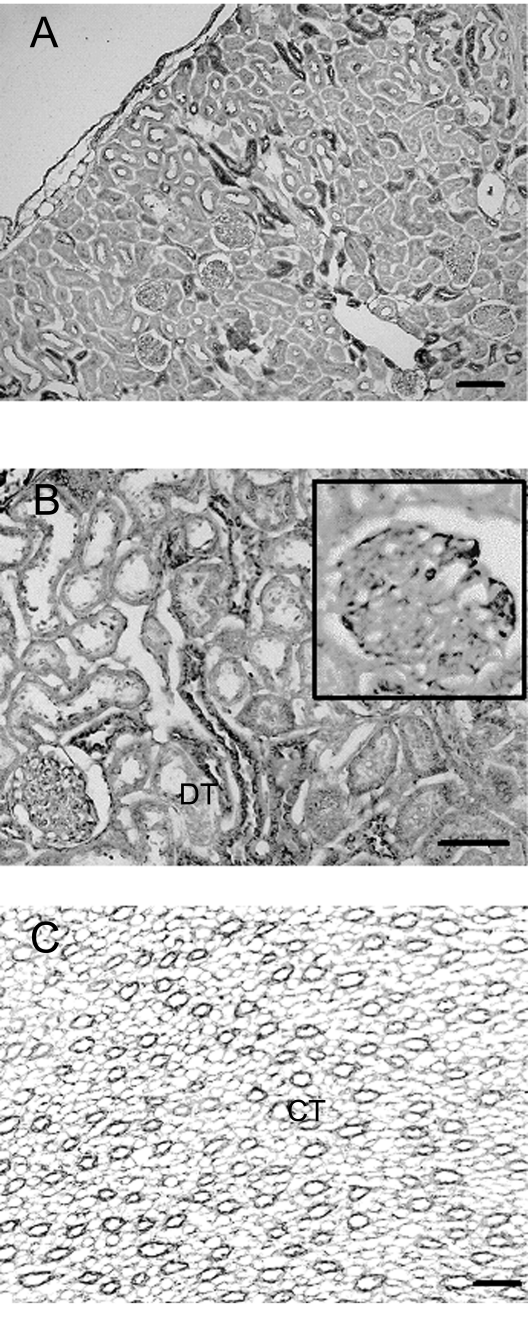

Figure 6

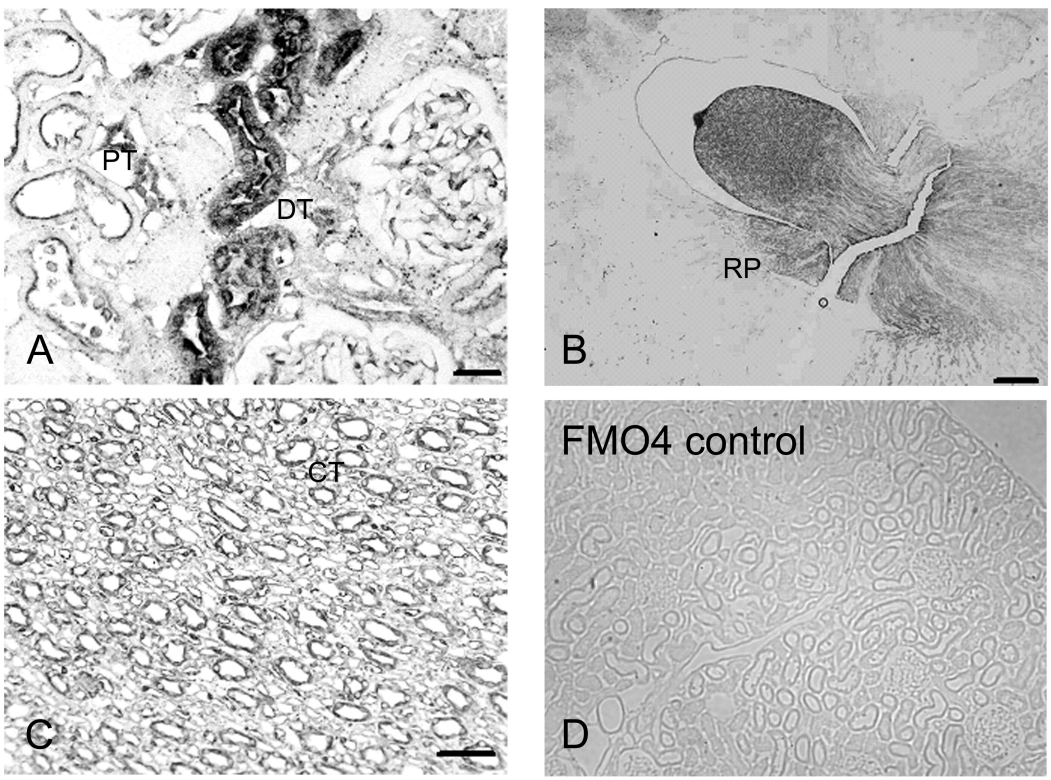

Figure 7

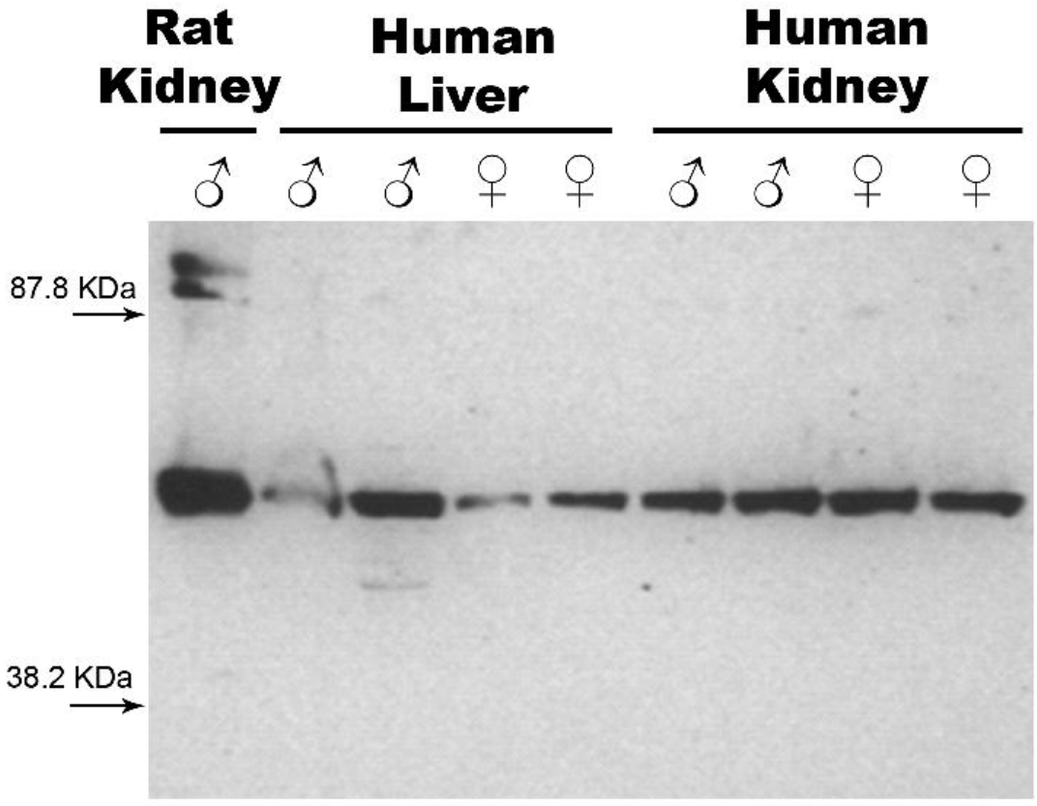
Rat Kidney
Human Liver
Human Kidney
♂ ♂ ♂ ♀ ♀ ♂ ♂ ♀ ♀
87.8 KDa
38.2 KDa

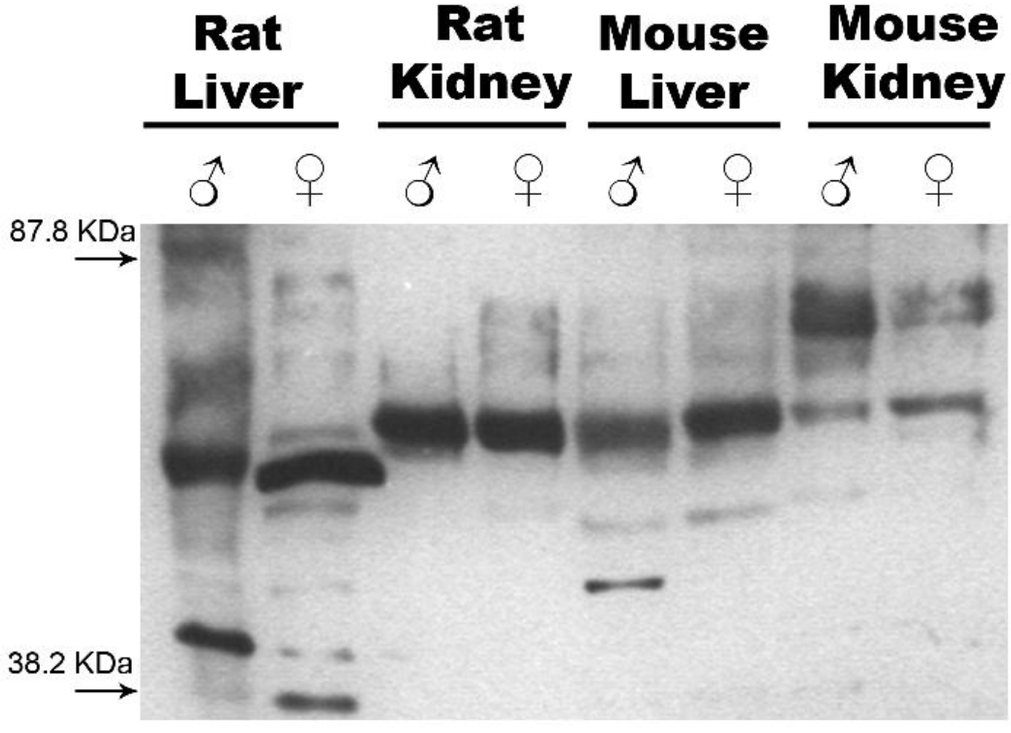
Rat Liver
Rat Kidney
Mouse Liver
Mouse Kidney
♂ ♀ ♂ ♀ ♂ ♀ ♂ ♀
87.8 KDa
38.2 KDa